Ether Lipid Biosynthesis Promotes Lifespan Extension and Enables Diverse Prolongevity Paradigms

Lucydalila Cedillo[a,b,c], Sainan Li[a,b], Fasih M. Ahsan[a,b,c], Sinclair Emans[a,b], Adebanjo Adedoja[a,b,c], Khoi Dao[d], Zhaozhi Li[e], Nicholas D. Peterson[f], Jeramie Watrous[d], Mohit Jain[d], Sudeshna Das[e], Read Pukkila-Worley[f], and Alexander A. Soukas[a,b,*]

[a]Center for Genomic Medicine and Diabetes Unit, Endocrine Division, Department of Medicine, Massachusetts General Hospital and Harvard Medical School, Boston MA 02114

[b]Broad Institute of Harvard and MIT, Cambridge, MA 02142

[c]Program in Biological and Biomedical Sciences, Division of Medical Sciences, Harvard Medical School, Boston, MA 02114

[d]Department of Medicine and Pharmacology, University of California San Diego, San Diego, CA 92093

[e]Biomedical Informatics Core, Massachusetts General Hospital and Harvard Medical School, Cambridge, MA 02139

[f]Program in Innate Immunity, Division of Infectious Diseases and Immunology, University of Massachusetts Medical School, Worcester, MA, 01655

*Corresponding Author: Alexander A. Soukas

Email: asoukas@mgh.harvard.edu

Author Contributions: Conceptualization, LC, AAS; Methodology, LC, SL, JW, MJ, AAS; Validation: LC, SL, FA, AAS; Formal Analysis: LC, JW, MJ, ZL, SD, AAS, NP, RPW; Investigation: LC, SL, FA, SE, AA, KD, JW, MJ, NP, RPW, AAS; Writing – Original Draft: LC, AAS; Writing – Review & Editing: LC, SL, FA, SE, AA, KD, JW, MJ, ZL, SD, NP, RPW, AAS; Visualization: LC, FA, ZL, SD, AAS; Supervision: AAS; Funding Acquisition: AAS.
Competing Interest Statement: The authors have no competing interests to declare.
Classification: Major: Biological Sciences. Minor: Genetics.
Keywords: metformin; aging; ether lipids; *C. elegans*; metabolism

This PDF file includes:

Main Text
Figures 1 to 4

Abstract

Biguanides, including the world's most commonly prescribed drug for type 2 diabetes, metformin, not only lower blood sugar, but also promote longevity in preclinical models. Epidemiologic studies in humans parallel these findings, indicating favorable effects of metformin on longevity and on reducing the incidence and morbidity associated with aging-related diseases, such as cancer. In spite of these promising observations, the full spectrum of the molecular effectors responsible for these health benefits remains elusive. Through unbiased genetic screening in *C. elegans*, we uncovered a novel role for genes necessary

for ether lipid biosynthesis in the favorable effects of biguanides. We demonstrate that biguanides govern lifespan extension via a complex effect on the ether lipid landscape requires enzymes responsible for both ether lipid biogenesis and polyunsaturated fatty acid synthesis. Remarkably, loss of the ether lipid biosynthetic machinery also mitigates lifespan extension attributable to dietary restriction, target of rapamycin (TOR) inhibition, and mitochondrial electron transport chain inhibition. Furthermore, overexpression of a single, key ether lipid biosynthetic enzyme, *fard-1*/FAR1, is sufficient to promote lifespan extension. These findings illuminate the ether lipid biosynthetic machinery as a novel therapeutic target to promote healthy aging.

Significance Statement

Metformin is the most widely used drug to treat patients with type 2 diabetes and extends lifespan in multiple species, yet the molecular targets responsible for these prolongevity benefits remain incompletely understood. To this end, we demonstrate that a subset of lipids, known as ether lipids, are necessary for biguanides' anti-aging effects and various other paradigms of lifespan extension. Strikingly, modulation of the machinery responsible for ether lipid biosynthesis is sufficient to stimulate lifespan extension, illuminating the possibility of using these lipids as therapeutic targets to promote healthy aging.

Main Text

Introduction

Metformin is the first line therapy for type 2 diabetes and the most frequently prescribed oral hypoglycemic medication worldwide (1). Human epidemiologic studies note an association between metformin use and decreased incidence of cancer (2, 3). In addition, metformin extends lifespan in invertebrate and vertebrate models (4-6), and therefore may reduce aging-related diseases in humans (7). Nonetheless, our understanding of the molecular pathways governing the health-promoting effects of metformin is only just beginning to emerge. Our previous work identified a conserved signaling axis connecting mitochondria, the nuclear pore complex, and mTORC1 inhibition that is required for metformin-mediated extension of lifespan in *C. elegans* and inhibition of growth in worms and human cancer cells (8). The energy sensor AMP-activated protein kinase (AMPK) is not necessary for metformin-induced growth inhibition in *C. elegans* but is required for the drug's prolongevity effects (4, 6, 9). Thus, the mechanisms by which metformin exacts its beneficial effects on health are likely to be branching and complex.

The importance of ether lipids, a major structural component of cell membranes, to aging and longevity is not well established. Ether lipids are involved in the maintenance of general membrane fluidity and in the formation of lipid rafts within microdomains, which are important for promotion of membrane fusion and cellular signaling (10-12). Ether lipids have broad roles in the regulation of cell

differentiation (13-16), cellular signaling (17, 18), and reduction of oxidative stress through their action as antioxidants (19-22). Humans deficient in ether lipid biogenesis suffer from rhizomelic chondrodysplasia punctata (RCDP), a rare genetic disorder, which results in skeletal and facial abnormalities, psychomotor retardation, and is uniformly fatal typically before patients hit their teens (23). Thus, evidence linking alterations in ether lipid levels to aging and longevity in humans is strictly correlative (24, 25).

Ether lipids, which are structurally distinct from canonical phospholipids, have a unique biosynthetic pathway through which a fatty alcohol is conjugated to the glycerol backbone at the sn-1 position via an ether linkage. Ether lipid precursors are first synthesized by enzymes associated with the membranes of peroxisomes (26-28). The main enzymes involved in ether lipid biosynthesis within the peroxisomal matrix are glyceronephosphate O-acyltransferase (GNPAT) and alkylglycerone phosphate synthase (AGPS). The peroxisomal membrane-associated fatty acyl-CoA reductase 1 (FAR1) supplies most of the fatty alcohols used to generate the ether linkage in the precursor, 1-O-alkyl-glycerol-3-phosphate. This precursor is then trafficked to the endoplasmic reticulum (ER) for unique acyl chain remodeling to produce various ether lipid products (29). In *C. elegans,* loss-of-function mutations of any of the three main enzymes involved in human ether lipid biosynthesis, *acl-7*/GNPAT, *ads-1*/AGPS, and *fard-1*/FAR1, results in an inability to produce ether linked lipids, as in humans (30). Worms and human cells deficient in ether lipids exhibit compensatory changes in phospholipid species, including increases in phosphatidylethanolamines and phosphatidylcholines containing saturated fatty acids (15, 31). However, in contrast to humans, ether lipid deficient nematodes develop normally, providing an opportunity to determine the biological roles of ether lipids in aging and longevity without developmental pleiotropies.

Here, we show that the ether lipid biosynthetic machinery underlies healthy aging in *C. elegan*s. Ether lipids are necessary for lifespan extension stimulated by metformin or the related biguanide phenformin. Metabolomic analysis indicates that phenformin treatment leads to changes in multiple ether lipids, primarily those with elongated and desaturated fatty acids in the sn-2 position. Interestingly, requirement for the ether lipid biosynthetic genes extends to multiple genetic paradigms used to study lifespan including defective mitochondrial electron transport function (*isp-1*), defective pharyngeal pumping/ caloric restriction (*eat-2*), and compromises in mTOR complex 1 activation (*raga-1*). Importantly, lack of ether lipid genes does not impact lifespan extension due to loss of function in the insulin receptor homolog *daf-2*, indicating that reductions in ether lipids does not simply cause non-specific sickness. Finally, overexpressing *fard-1*, the enzyme that supplies all the fatty alcohols for ether lipid biogenesis in *C. elegans*, extends lifespan, suggesting that an increase in ether lipids alone is sufficient to promote healthy aging.

Results

Genes Responsible for Ether Lipid Biosynthesis are Necessary for Biguanide-Induced Lifespan Extension. From a previous RNAi screen of ~1000 metabolic genes for knockdowns that interfere with the growth-inhibitory properties of metformin in *C. elegans* (8), we identified several genes required for ether lipid biosynthesis. Ether lipids are distinguished from canonical phospholipids as the latter contain exclusively fatty acids conjugated to glycerol, whereas ether lipids contain a fatty alcohol conjugated to the glycerol backbone at the sn-1 position via an ether linkage (Fig. 1*A*). Confirming our screen results, RNAi knockdown of two genes involved in ether lipid biosynthesis, *fard-1* and *acl-7*, results in significant resistance to biguanide induced growth inhibition (Fig. S1*A*). Our lab has previously demonstrated that biguanide effects on growth in *C. elegans* share significant overlap mechanistically with the machinery by which metformin extends lifespan in the worm (8). Indeed, loss-of-function mutations in any of three genes encoding enzymes required for ether lipid biosynthesis, *fard-1*, *acl-7* or *ads-1*, significantly suppresses lifespan extension induced by both metformin and the related biguanide phenformin (Fig. 1 *B*-*G*, Dataset S1 for tabular survival statistics and biological replicates). Confirming that these mutations confer resistance to metformin by compromising ether lipid synthetic capacity, RNAi knockdowns of *fard-1* and *acl-7* also partially impair lifespan extension promoted by phenformin (Fig. S1 *B* and *C*). Studies from this point forward are presented predominantly with phenformin because 1) phenformin is known to be more readily absorbed without need for a specific transporter, unlike metformin, (8, 32, 33) and 2) our experience indicates more consistent lifespan extension with phenformin in *C. elegans*.

Because ether lipids are a major structural component of cell membranes, one possibility is that deficiencies in ether lipid synthesis compromises drug action by reducing biguanide bioavailability in the worm. To test this, we compared the relative levels of biguanides present in vehicle- and biguanide- treated wild type to the three ether lipid synthesis mutants by LC-MS/MS. A comparison of normalized concentrations of phenformin across all four strains shows that phenformin abundance is significantly higher in phenformin-treated samples relative to the corresponding vehicle-treated controls, and that phenformin levels are similar across wild type and all three ether lipid mutant strains (Fig. 1*H* and Fig. S1*D*). Similar results were obtained when comparing levels of metformin wild type and ether lipid mutant animals (Fig. 1*I* and Fig. S1*E*). Thus, deficiency in ether lipid synthesis does not significantly impact uptake or clearance of biguanides in *C. elegans.*

Phenformin Induces Changes in Ether Lipid Metabolite Levels. We reasoned that if biguanides require ether lipid biosynthesis to promote lifespan extension that phenformin may promote changes in abundance of one or several ether lipids. To

174 investigate the impact of biguanides on ether lipids at a high level, we first utilized
175 gas chromatography-mass spectrometry (GC-MS) analysis. GC-MS recapitulates
176 the observation that *fard-1* mutants show absence of 18-carbon containing alkenyl
177 ether lipids (also known as plasmalogens) and an accumulation of stearic acid
178 (18:0) relative to wild type controls (Fig. 2 *A* and *B*). We then asked if phenformin
179 impacts the levels of stearic acid and 18-carbon alkenyl ether lipids in wild type
180 animals and if those corresponding changes are absent in *fard-1* mutants.
181 Strikingly, phenformin-treated wildtype worms display a significant increase in 18-
182 carbon alkenyl ether lipids (also known as plasmalogens, as in Fig. 1*A*) versus
183 vehicle, whereas no such increase is evident in drug treated *fard-1* worms (Fig.
184 2*C*). In addition, relative proportions of stearic acid levels within the total fatty acid
185 pool are significantly increased in *fard-1* mutants treated with phenformin versus
186 vehicle treated *fard-1* controls. In comparison, the relative proportion of stearic acid
187 does not rise in phenformin treated wild type animals, suggesting that stearate is
188 being utilized for ether lipid production (Fig. 2*D*). We conclude that phenformin
189 treatment leads to an overall increase of ether lipid levels in *C. elegans*.
190 To investigate changes across the entire landscape of alkyl and alkenyl
191 ether lipids in response to phenformin, we utilized LC-MS/MS lipidomics. This
192 method detected 270 alkyl and alkenyl ether lipids (Fig. 2*E*, and Dataset S2). After
193 filtering for ether lipids significantly altered in abundance in response to
194 phenformin, we implemented a spectral clustering model to visualize the difference
195 of the average normalized value in wild type as compared to the three ether lipid
196 mutants *fard-1*, *acl-7*, and *ads-1*. Two clusters of ether lipids have a significant
197 change in metabolite concentrations in wild type worms but not *fard-1*, *acl-7*, and
198 *ads-1* mutants treated with phenformin compared to vehicle (Fig. 2*E* and Table S1,
199 clusters 1 and 3). As an orthogonal strategy, we utilized a linear model to identify
200 ether lipids with a significant change in abundance between vehicle and biguanide
201 treatment in wild type animals, without a corresponding change in the ether lipid
202 deficient mutants (Fig. 2*F*). These two independent models 1) had strong overlap
203 among ether lipids increased in response to phenformin (of 14 ether lipids from
204 cluster 1 spectral clustering (Fig. 2*E*) and 13 increased from the linear model (Fig.
205 2*F*), 12 are overlapping, Table S1) and 2) indicate an ether lipid metabolite
206 signature of phenformin treatment that is prevented in ether lipid biosynthetic
207 mutants.
208 Three important features are evident from analysis of the lipidomics data.
209 First, classic ether lipids containing non-oxidized fatty alcohols that significantly
210 increase in response to phenformin treatment are far more abundant than ether
211 lipids decreased in abundance (by mass counts, Fig. 2*F* and Dataset S2). In
212 particular, the most increased ether lipid, phosphatidylglycerol(P-
213 18:0/18:2(9Z,12Z)), is more abundant following phenformin treatment than all of
214 the other ether lipids decreased in abundance in aggregate (8.2 million mass
215 counts versus 4.4 million, respectively). Second, 11 of the 15 ether lipids increased
216 in abundance from both analyses are alkenyl-type (plasmalogen) ether lipids,
217 including those most abundant by mass counts. This data agrees with our GC/MS

218 data (Fig. 2*C*) indicating an increase in plasmalogen-type ether lipid types in
219 response to phenformin. Third, examination of the molecular identities of the ether
220 lipids increased in response to phenformin indicates that 9 of 15 harbor elongated,
221 polyunsaturated fatty acids in the sn-2 position, suggesting a potential role for the
222 enzymes implicated in the biogenesis of these fatty acids in metformin action.
223
224 **Phenformin Stimulates Peroxisomal Localization of FARD-1**. In order to begin
225 to understand the governance of ether lipid biosynthesis by biguanides, we
226 generated *C. elegans* expressing a FARD-1::RFP translational reporter from an
227 extrachromosomal array under its own promoter (Fig. S2*A*). Imaging of these
228 worms reveals that FARD-1 is expressed in intestine and appears to localize
229 nearby structures resembling lipid droplets (Fig. S2*B*). Given that ether lipid
230 biogenesis is reported to occur in peroxisomes, we crossed the FARD-1::RFP
231 reporter to an animal bearing a GFP reporter that illuminates peroxisomes in
232 intestine (GFP fused to a C-terminal peroxisomal targeting sequence 1(PTS1)).
233 FARD-1::RFP fluorescence partially overlaps with peroxisomally-targeted GFP in
234 intestine (Fig. S2*C*). Compellingly, treatment with phenformin leads to an increase
235 in overlap between FARD-1::RFP and GFP::PTS1 (Pearson's R value=0.84)
236 relative to vehicle treated controls (Pearson's R value=0.73) (Fig. S2*C*). The same
237 trend is present in another biological replicate where the Pearson's correlation
238 value for the overlap between GFP and RFP in the phenformin treated transgenic
239 is R= 0.57 versus R= 0.39 in vehicle. These results suggest that biguanides may
240 govern ether lipid biosynthesis by recruiting greater amounts of FARD-1 to
241 peroxisomes.
242 Curiously, expression of mRNAs encoding FARD-1, ACL-7, and ADS-1 are
243 all decreased or unchanged in abundance upon treatment with biguanide via
244 quantitative real time RT-PCR (Fig. S2 *D-I*). A parallel decrease in overall levels of
245 the FARD-1::RFP transgene was seen with phenformin treatment (Fig. S2*J*).
246 These seemingly paradoxical data are consistent with the possibility that
247 biguanides increase activity of ether lipid biosynthetic pathways post-
248 translationally given that ether lipids have been previously reported to exert
249 negative feedback on protein levels of FARD-1 (Honsho et al., 2010).
250 We surmised that if ether lipid synthesis is occurring principally in the
251 peroxisome and that peroxisomal localization of FARD-1 was required for the
252 prolongevity response to biguanides, that disruption of peroxisomal protein
253 targeting should also impair phenformin-stimulated lifespan extension. Indeed,
254 either *prx-5* or *prx-19* RNAi impair lifespan extension prompted by phenformin fully
255 or partially, respectively (Fig. 3 *A* and *B*). PRX-5 is involved in protein import into
256 the peroxisome matrix and PRX-19 is involved in proper sorting of proteins for
257 peroxisomal biogenesis. Thus, either disruption of ether lipid biosynthetic
258 machinery or of a principal site of ether lipid biosynthesis impairs phenformin's
259 prolongevity benefit.
260

Functional Genomics Implicates Fatty Acid Elongases and Desaturases in Biguanide-Mediated Lifespan Extension. Analysis of specific ether lipids significantly altered in abundance in response to phenformin (Fig. 2*F*) indicated 13 ether lipids with long and/or polyunsaturated fatty acids at the sn-2 position. These types of fatty acids are largely synthesized endogenously in *C. elegans* by fatty acid desaturases and fatty acid elongases (34, 35) (Fig. 3*C*). We reasoned that these desaturases and elongases may also contribute mechanistically to biguanide mediated lifespan extension. Indeed, RNAi knockdown of three fatty acid desaturases and two fatty acid elongases in phenformin-treated *C. elegans* blunted phenformin-stimulated lifespan extension relative to empty vector controls (Fig. 3 *D-H*). Notably, these five genes all contribute to the production of fatty acids 18-20 carbons in length with three or more double bonds. Although knockdown of fatty acid desaturases and elongases in *C. elegans* results in inherent lifespan extension on vehicle relative to wild type controls on empty vector RNAi as has been previously reported (36, 37), these RNAi knockdown completely mitigate phenformin-driven lifespan extension (Fig. 3 *D-H*). These results suggest that fatty acid desaturases and elongases promote biguanide-mediated lifespan extension through contribution of long and polyunsaturated fatty acids to the synthesis of ether lipids.

Genes Involved in Ether Lipid Biosynthesis Are Required in Multiple Longevity Paradigms. Given the critical role of ether lipids in the response to biguanides, we next endeavored to determine whether these molecules also play a broader role in diverse longevity paradigms involving metabolic or nutrient-sensing pathways. *C. elegans* mutant strains that exhibit 1) reduced mitochondrial function (*isp-1*), 2) disrupted mTORC1 signaling (*raga-1*), 3) abnormal pharyngeal pumping (*eat-2*), or 4) inhibition of insulin/insulin-like growth factor-1 signaling (*daf-2*), all result in extension of lifespan (38-41). To determine whether requirement for the ether lipid biosynthetic machinery in aging generalizes to other lifespan extension paradigms, we knocked down all three ether lipid biosynthetic enzymes by RNAi in wild type *C. elegans* and four long-lived genetic mutants: *raga-1*, *isp-1*, *eat-2*, and *daf-2*. Knockdown of *fard-1*, *acl-7*, and *ads-1* by RNAi results in suppression of lifespan extension in *isp-1*, *raga-1*, and *eat-2* mutants (Fig. 4 *A-C*). However, knockdown of ether lipid synthesis genes by RNAi did not impact lifespan extension in *daf-2* mutants (Fig. S3*A*). Thus, the ether lipid biosynthetic machinery plays a broad role in lifespan extension, and, importantly, does not simply cause non-selective sickness.

Overexpression of FARD-1 is Sufficient to Promote Lifespan Extension. To determine whether stimulation of ether lipid biosynthesis is sufficient to prompt lifespan extension, we tested the effect of *fard-1* overexpression (*oe*) on *C. elegans* lifespan. Strikingly, *fard-1*(*oe*) alone results in significant lifespan extension (Fig. 4*D*). This result is similar between two independent *fard-1*(*oe*) transgenic lines (Fig 4*E*). To confirm that *fard-1*(*oe*) lifespan extension is dependent upon ether lipid

305 biosynthesis, we knocked down *fard-1*, *acl-7*, and *ads-1* by RNAi in the *fard-1*(*oe*).
306 As predicted, knockdown of three ether lipid biosynthetic enzymes leads to
307 significant suppression of *fard-1*(*oe*) lifespan extension (Fig. 4*F* and Fig. S3 *B* and
308 *C*).
309 To determine the lifespan extension attributable to *fard-1* overexpression
310 shares any genetic dependencies of biguanide-mediated longevity, we
311 independently knocked down *skn-1*/*Nrf2*, *aak-2*/AMPK and *daf-16*/*FoxO* by RNAi
312 in a *fard-1*(*oe*) background. While *skn-1*/*Nrf2* and *aak-2*/AMPK have previously
313 been demonstrated to be necessary for metformin-stimulated lifespan extension,
314 *daf-16/FoxO* has not (6, 42). Lifespan extension attributable to *fard-1*(*oe*) is
315 suppressed by these three gene knockdowns (Fig. 4 *G-I*), indicating that it is
316 mechanistically similar but not identical to biguanide-mediated lifespan extension
317 (4, 6). In aggregate, these results support the notion that ether lipids are an
318 important requirement in multiple, diverse longevity paradigms, and further that
319 *fard-1*(*oe*) is a genetically distinct lifespan extension paradigm in *C. elegans.*
320
321 **Discussion**
322
323 In an unbiased RNAi screen of ~1000 metabolic genes, we identified ether
324 lipid biosynthesis as critical to the longevity-promoting effects of metformin in *C.*
325 *elegans*. Our results show that the biguanides metformin and phenformin promote
326 lifespan extension through complex effects on the landscape of ether lipids, an
327 effect that may be mediated by governance of peroxisomal localization of the sole
328 enzyme capable of synthesizing fatty alcohols, FARD-1. Two observations
329 demonstrate the broad importance of these findings: 1) the ether lipid biosynthetic
330 machinery is also required for multiple, diverse paradigms of lifespan extension,
331 and 2) *fard-1* overexpression alone is sufficient to promote lifespan extension.
332 Thus, ether lipids form a heretofore unappreciated dimension of lifespan
333 modulation, and are sufficient to support healthy aging through multiple, central
334 longevity effectors.
335 Differences in ether lipid abundance and composition are correlated with
336 diseases of aging. The uniform lethality associated with human genetic ether lipid
337 deficiency, as in the case of patients diagnosed with RCDP and Zellweger
338 syndrome, has made it difficult to study the role of ether lipids in aging and aging-
339 associated diseases (43-46). Nonetheless, observational studies suggest
340 decreases in certain plasmalogen species in Alzheimer's Disease, suggesting a
341 link between ether lipids and aging-related pathologies (47-49). Ether lipids have
342 conflicting roles in cancer; while loss of the ether lipid biosynthetic machinery
343 profits renal and ovarian cancer cell survival by enhancing resistance to ferroptosis
344 (50), in other contexts, ether lipid deficiency results in impaired pathogenicity in
345 breast and ovarian cancer cells (31). Cancer cells generally have higher levels of
346 ether lipids compared to normal cells, leading others to suggest that ether lipids
347 confer pro-survival benefit (31, 51, 52). However, certain ether lipid species have
348 also been reported to have anti-tumor properties (53, 54). Thus, akin to the results

349 we present here, it is critical to understand ether lipids in context, and the impact
350 of specific ether lipid species rather than the whole class *en masse* to understand
351 which may play a beneficial versus detrimental role in health.

352 Studies in long-lived animal models suggest there is an association
353 between ether lipid content and animal longevity, such as in the naked mole-rat
354 (*Heterocephalus glaber*) (55) and the mud clam *Arctica islandica* (56). Higher
355 plasmalogen levels in naked mole-rat tissues versus mice, are speculated to
356 contribute to protection of cellular membranes via a reduction of oxidative stress
357 (55). Similarly, exceptionally long-lived humans harbor higher levels of
358 phosphatidylcholine-derived, short chained alkyl ether lipids and a lower levels of
359 phosphatidylethanolamine-derived longer chained plasmalogens (25), but these
360 associations are of unclear functional significance. Although it is clear that ether
361 lipid deficiency in *C. elegans* both prevents normal lifespan (30) and longevity
362 downstream of mitochondrial dysfunction, mTOR deficiency, caloric restriction,
363 and biguanides alike, the precise molecular species conferring this activity remains
364 unclear. Each of these longevity paradigms have features of nutrient deficiency or
365 the response to nutrient deficiency, so it is possible that ether lipids are at least
366 part of the common effector arm conferring benefit in aging to various forms of
367 metabolic stress.

368 Our results suggest that ether lipids containing long and/or desaturated fatty
369 acids at the sn-2 position may be essential to the health promoting effects of
370 biguanides. Although we see major shifts in abundance of alkenyl ether lipids,
371 genetic evidence of necessity of ether lipids, and requirement for the synthesis of
372 mono- and poly-unsaturated fatty acids in biguanide-induced longevity,
373 determination of the specific lipids necessary for promoting healthy aging awaits
374 the ability to modulate the level of specific ether lipid species. Further, disruption
375 of ether lipid biosynthesis has been shown to increase the proportion of stearate
376 (18:0) and other saturated fatty acids (30), and our own data show that some ether
377 lipids increase in abundance while others decrease in response to phenformin.
378 Thus, at this time, we cannot rule out the possibility that biguanide-stimulated
379 alterations in ether lipid biosynthesis serves to divert accumulation of more “toxic”
380 lipid species that are detrimental to lifespan. This will require a deeper
381 understanding of the regulation of specific steps dictating the synthesis and
382 modification of ether lipids of different fatty alcohol and fatty acid composition.

383 Our data are the first to suggest that peroxisomal trafficking of the fatty
384 alcohol reductase FARD-1 could be a mechanism for regulation of favorable ether
385 lipids in aging. Indeed, our observation that FARD-1 mRNA and protein levels are
386 decreased by biguanides is consistent with the suggestion that 1) biguanides
387 promote ether lipid biogenesis by promoting post-translational FARD-1 activation
388 and 2) previous work demonstrating that higher levels of ether lipids promotes
389 proteasomal degradation of peroxisomal Far1 protein (57). Modulation of the
390 peroxisomal localization of FARD-1 may provide the first clue to identify the precise
391 ether lipids necessary to promote longevity.

In aggregate, data presented here indicate that ether lipid biosynthesis plays a broader role in aging than previously described. The necessity of the ether lipid machinery in metformin- and phenformin-stimulated lifespan extension and in multiple longevity paradigms indicates that ether lipids serve as a lynchpin through which lifespan is modulated (Fig 4*J*). Our demonstration that overexpression of FARD-1 alone results in lifespan extension provides an exciting opportunity to identify ether lipids that promote health and the effector mechanisms through which they act. Finally, these results support the exciting possibility that modulation of ether lipids pharmacologically or even dietarily may provide a new potential therapeutic target in aging and aging-related diseases.

Materials and Methods

C. elegans genetics. Strains were maintained at 20°C. The following strains were used in this study: N2 (wild-type strain), BX275 *fard-1*(*wa28*), BX259 *acl-7*(*wa20*), BX10 *ads-1*(*wa3*), CB1370 *daf-2*(*e1370*), MQ989 *isp-1*(*qm150*), VC533 *raga-1*(*ok701*), DA465 *eat-2*(*da465*), MGH48 *mgIs43*[*ges-1p*::GFP::PTS1]. For *fard-1* overexpression, the following strains were generated: MGH471 *alxEx122*[*fard-1p*::FARD-1::mRFP::HA *myo-2p*::GFP] (*fard-1 oe1*), MGH472 *alxEx124*[*fard-1p*::FARD-1::mRFP::HA *myo-2p*::GFP] (*fard-1 oe2*).

Statistical analysis of metabolomics data. Mass integration for 270 ether lipids was extracted from scan mode LC-MS/MS. Non-variant lipids were excluded from subsequent analyses. We performed one-way ANOVA analysis using the *anova* function from the *stats* package to test the hypothesis that drug uptake was similar in wildtype (N2) and ether lipid mutants. Shapiro-Wilk test (*shapiro.test*) and *bptest* functions from the *stats* package were used to check normality of data and homoscedasticity of the residuals, respectively. To explore whether the drug was entering the samples, we used a linear model to estimate the drug uptake (with corresponding confidence intervals) for wild type and ether lipid mutants as follows,

$$\text{compound_concentration} = \beta_0 + \beta_1 * \text{sample group} + \varepsilon$$

where:

β_0 =intercept

β_1 =group effect

ε =noise

Next, we identified phenformin signatures that were induced by the drug and prevented in the lipid mutants using spectral clustering, which is a machine-learning algorithm to identify groups of compounds with similar concentration profiles. After selecting for 270 ether lipids, spectral clustering was performed using the *SNFtool* package (version 2.3.0) with k = 6 based on the difference between average log-normalized values of phenformin treated samples and the

436 vehicle. We further estimated the effect size and significance of the ether lipids in
437 the phenformin treated wild type and mutant samples compared to the vehicle
438 using the *limma* package (version 3.44.3).
439
440 **Generation of *fard-1 C. elegans* transgenic lines.** For FARD-1 expression, the
441 entire genomic sequence of the *fard-1* locus (3659 bp), including introns and
442 exons, plus 4910 bp of promoter were amplified and cloned into a modified Fire
443 vector driving *fard-1* fused to mRFP and a HA epitope tag at the C-terminus. The
444 following cloning primers were used:
445
446 forward: 5'- TGCATGCCTGCAGGTCGACTTTGACAAAAGTTCTGTTGCCG -3'
447 and
448 reverse:
449 5'- TTTGGGTCCTTTGGCCAATCGCTTTTTTGAAGATACCGAGAATAATCC -3'.
450
451 The FARD-1 overexpression construct was injected at 10 ng/uL (alxEx122) and 18
452 ng/uL (alxEx124) into the gonad of wild type adult animals with salmon sperm DNA
453 as a carrier and 1.5 ng/uL *myo-2p*::GFP as a co-injection marker.
454
455 **Longevity assays.** Lifespan analysis was conducted at 20°C, as previously
456 described (58). Briefly, synchronized L1 animals were seeded onto NGM (for
457 mutant treatment) or RNAi plates (for RNAi) and allowed to grow until the L4-young
458 adult (YA) stage. On day 0 of adulthood as indexed in the figure legend, ~50-60
459 L4/YA worms per plate (unless otherwise noted) were transferred onto fresh NGM
460 or RNAi plates. These NGM and RNAi plates were supplemented with 30 µM and
461 100 µM 5-fluorodeoxyuridine (FUdR) to suppress progeny production,
462 respectively. For biguanide treatment, about ~55-60 synchronized L1 animals
463 (unless otherwise noted) were seeded onto plates containing 50 mM metformin or
464 4.5 mM phenformin. At the L4/YA stage, these worms were transferred to plates
465 containing biguanide treatment and FUdR for the remainder of their life. Dead
466 worms were counted every other day. Statistical analysis was performed with
467 online OASIS2 resources (59).
468
469 **RNA interference (RNAi) assays.** RNAi clones were isolated from a genome-
470 wide *E. coli* RNAi library, sequence verified, and fed to animals as described (60).
471 RNAi feeding plates (6 cm) were prepared using a standard NGM recipe with 5
472 mM isopropyl-B–D-thiogalactopyranoside and 200 µg/ml carbenicillin. RNAi
473 clones were grown for 15 hours in Luria Broth (LB) containing 100 µg/ml
474 carbenicillin with shaking at 37°C. The stationary phase culture was then collected,
475 concentrated through centrifugation, the supernatant was discarded, and the pellet
476 was resuspended in LB to 20% of the original culture volume; 250 µl of each RNAi
477 clone concentrate was added to RNAi plates and allowed to dry at least 24 hours
478 prior to adding biguanide. Drug treatment was added to seeded RNAi plates and
479 allowed to dry at least 3 hours before adding worms.

480
481 **Quantification and statistical analysis.** Statistical analyses were performed
482 using Prism (GraphPad Software). The statistical differences between control and
483 experimental groups were determined by two-tailed students *t*-test (two groups),
484 one-way ANOVA (more than two groups), or two-way ANOVA (two independent
485 experimental variables), with corrected P values < 0.05 considered significant. The
486 log rank test was used to determine significance in lifespan analyses using online
487 OASIS2.
488
489 **GC/MS lipidomics.** Lipid extraction and GC/MS of extracted, acid-methanol-
490 derivatized lipids was performed as described previously (61, 62). Briefly, 5000
491 synchronous mid-L4 animals were sonicated with a probe sonicator on high
492 intensity in a microfuge tube in 100-250 microliters total volume. Following
493 sonication, lipids are extracted in 3:1 methanol: methylene chloride following the
494 addition of acetyl chloride in sealed borosilicate glass tubes, which were then
495 incubated in a 75°C water bath for 1 hour. Derivatized fatty acids and fatty alcohols
496 were neutralized with 7% potassium carbonate, extracted with hexane, and
497 washed with acetonitrile prior to evaporation under nitrogen. Lipids were
498 resuspended in 200 microliters of hexane and analyzed on an Agilent GC/MS
499 equipped with a Supelcowax-10 column as previously described (61). Fatty acids
500 and alcohols were indicated as the normalized peak area of the total of derivatized
501 fatty acids and alcohols detected in the sample.
502
503 **LC/MS-MS lipidomics.** Wildtype, *fard-1*, *acl-7*, and *ads-1* worm mutants were
504 collected using conditions that enabled our reported longevity phenotypes. Briefly,
505 collection for LC/MS-MS processing comprised of 3 replicates of these 4 strains
506 that were independently treated with vehicle (ddH_2O), 50mM metformin, and
507 4.5mM phenformin on 10cm NGM plates. A set of untreated worms were included
508 for optimization of LC-MS/MS processing, for a total of 39 samples. A total of
509 ~6,000 animals (2 x 10cmM plates, 3,000 worms per plate) were utilized per
510 sample. These worms were washed with M9 (4x), concentrated into 200uL of M9,
511 and then flash frozen with liquid nitrogen in 1.5mL Eppendorf microcentrifuge
512 tubes. Worm pellets were transferred to 2 mL impact resistant homogenization
513 tubes containing 300 mg of 1 mm zirconium beads and 1 mL of 90:10
514 ethanol:water. Using a Precellys 24 tissue homogenizer, samples were
515 homogenized in three 10 second cycles at 6400 Hz followed by 2 minutes of
516 sonication. Samples were then placed at -20 °C for one hour to facilitate protein
517 precipitation. Samples were transferred to 1.5 mL microfuge tubes and centrifuged
518 at 14,000 g for 10 minutes at 4 °C. After centrifugation, 120 μL of supernatant was
519 dried *in vacuo* and resuspended in 120 μL of 80:20 methanol:water containing
520 internal standards 1 ng/μL CUDA and 1 ng/μL MAPCHO-12-d38. Lipidomic data
521 was acquired by injecting 20 μL of sample onto a Phenomenex Kinetex F5 2.6 μm
522 (2.1 x 100 mm) column at 40 °C and flowing at 0.35 mL/min. Metabolites were
523 eluted using (A) water containing 0.1% formic acid and (B) acetonitrile:isopropanol

524 (50:50) containing 0.1% formic acid using the following gradient: 0% B from 0-1
525 min, 0-50% B from 1-6 mins, 50-100% B from 6 to 17 minutes and 100% B hold
526 from 17- 20 mins. Compounds were detected using a Thermo Scientific QExactive
527 Orbitrap mass spectrometer equipped with a heated electrospray ionization (HESI)
528 source operating in positive and negative ion mode with the following source
529 parameters: sheath gas flow of 40 units, aux gas flow of 15 units, sweep gas flow
530 of 2 units, spray voltage of +/-3.5 kV, capillary temperature of 265°C, aux gas temp
531 of 350°C, S-lens RF at 45. Data was collected using an MS1 scan event followed
532 by 4 DDA scan events using an isolation window of 1.0 m/z and a normalized
533 collision energy of 30 arbitrary units. For MS1 scan events, scan range of m/z 100-
534 1500, mass resolution of 17.5k, AGC of $1e^6$ and inject time of 50 ms was used. For
535 tandem MS acquisition, mass resolution of 17.5 k, AGC $5e^5$ and inject time of 80
536 ms was used. Data was collected using Thermo Xcalibur software (version
537 4.1.31.9) and analyzed using Thermo QualBrowser (version 4.1.31.9) as well as
538 MZmine 2.36.
539
540 **Acknowledgments**
541
542 We thank Dr. Yuyao Zhang, Dr. Yifei Zhou, Talia Hart, Luke Murphy, and Dr.
543 Armen Yerevanian for discussions and constructive criticisms. This work was
544 funded by NIH/NIA Grants R01AG058259 and R01AG69677 (to A.A.S), by the
545 Weissman Family MGH Research Scholar Award (to A.A.S.), by a NSF GRFP
546 Award 1000253984 (to L.C.), and by NIH/NIAID R01AI130289 (to R.P.W.). Thanks
547 to the NIH/NIDDK-funded NORC of Harvard (P30DK040561) and the NIH/NIDDK-
548 funded Boston-Area DERC (P30DK057521) for core services. Some strains were
549 provided by the CGC, funded by the NIH Office of Research Infrastructure
550 Programs (P40OD010440), and the *C. elegans* Knockout Consortium. Fig. 1*A*, 3*C*,
551 and 4*J* were created with BioRender.com.
552
553 **References**
554
555 1. S. E. Inzucchi *et al.*, Management of hyperglycaemia in type 2 diabetes: a
556 patient-centered approach. Position statement of the American Diabetes
557 Association (ADA) and the European Association for the Study of
558 Diabetes (EASD). *Diabetologia* **55**, 1577-1596 (2012).
559 2. J. M. Evans, L. A. Donnelly, A. M. Emslie-Smith, D. R. Alessi, A. D. Morris,
560 Metformin and reduced risk of cancer in diabetic patients. *Bmj* **330**, 1304-
561 1305 (2005).
562 3. P. Yuan *et al.*, Phenformin enhances the therapeutic benefit of
563 BRAFV600E inhibition in melanoma. *Proceedings of the National*
564 *Academy of Sciences* **110**, 18226-18231 (2013).
565 4. F. Cabreiro *et al.*, Metformin retards aging in C. elegans by altering
566 microbial folate and methionine metabolism. *Cell* **153**, 228-239 (2013).

567 5. A. Martin-Montalvo *et al.*, Metformin improves healthspan and lifespan in
568 mice. *Nature communications* **4**, 1-9 (2013).
569 6. B. Onken, M. Driscoll, Metformin induces a dietary restriction–like state
570 and the oxidative stress response to extend C. elegans healthspan via
571 AMPK, LKB1, and SKN-1. *PloS one* **5**, e8758 (2010).
572 7. N. Barzilai, J. P. Crandall, S. B. Kritchevsky, M. A. Espeland, Metformin as
573 a tool to target aging. *Cell metabolism* **23**, 1060-1065 (2016).
574 8. L. Wu *et al.*, An ancient, unified mechanism for metformin growth inhibition
575 in C. elegans and cancer. *Cell* **167**, 1705-1718. e1713 (2016).
576 9. J. Chen *et al.*, Metformin extends C. elegans lifespan through lysosomal
577 pathway. *Elife* **6**, e31268 (2017).
578 10. P. E. Glaser, R. W. Gross, Plasmenylethanolamine facilitates rapid
579 membrane fusion: a stopped-flow kinetic investigation correlating the
580 propensity of a major plasma membrane constituent to adopt an HII phase
581 with its ability to promote membrane fusion. *Biochemistry* **33**, 5805-5812
582 (1994).
583 11. D. Komljenovic *et al.*, Disruption of blood-testis barrier dynamics in ether-
584 lipid-deficient mice. *Cell and tissue research* **337**, 281-299 (2009).
585 12. S.-J. Marrink, A. E. Mark, Molecular view of hexagonal phase formation in
586 phospholipid membranes. *Biophysical journal* **87**, 3894-3900 (2004).
587 13. S. S. Davies *et al.*, Oxidized alkyl phospholipids are specific, high affinity
588 peroxisome proliferator-activated receptor γ ligands and agonists. *Journal*
589 *of Biological Chemistry* **276**, 16015-16023 (2001).
590 14. F. Facciotti *et al.*, Peroxisome-derived lipids are self antigens that
591 stimulate invariant natural killer T cells in the thymus. *Nature immunology*
592 **13**, 474-480 (2012).
593 15. C. Rodemer *et al.*, Inactivation of ether lipid biosynthesis causes male
594 infertility, defects in eye development and optic nerve hypoplasia in mice.
595 *Hum Mol Genet* **12**, 1881-1895 (2003).
596 16. A. Teigler, D. Komljenovic, A. Draguhn, K. Gorgas, W. W. Just, Defects in
597 myelination, paranode organization and Purkinje cell innervation in the
598 ether lipid-deficient mouse cerebellum. *Hum Mol Genet* **18**, 1897-1908
599 (2009).
600 17. A. K. Thukkani *et al.*, Reactive chlorinating species produced during
601 neutrophil activation target tissue plasmalogens: production of the
602 chemoattractant, 2-chlorohexadecanal. *J Biol Chem* **277**, 3842-3849
603 (2002).
604 18. C. J. Albert *et al.*, Eosinophil peroxidase-derived reactive brominating
605 species target the vinyl ether bond of plasmalogens generating a novel
606 chemoattractant, alpha-bromo fatty aldehyde. *J Biol Chem* **278**, 8942-
607 8950 (2003).
608 19. O. H. Morand, R. A. Zoeller, C. R. Raetz, Disappearance of plasmalogens
609 from membranes of animal cells subjected to photosensitized oxidation. *J*
610 *Biol Chem* **263**, 11597-11606 (1988).

611 20. R. A. Zoeller, O. H. Morand, C. R. Raetz, A possible role for plasmalogens
612 in protecting animal cells against photosensitized killing. *J Biol Chem* **263**,
613 11590-11596 (1988).
614 21. D. Reiss, K. Beyer, B. Engelmann, Delayed oxidative degradation of
615 polyunsaturated diacyl phospholipids in the presence of plasmalogen
616 phospholipids in vitro. *Biochem J* **323 (Pt 3)**, 807-814 (1997).
617 22. R. Maeba, Y. Sawada, H. Shimasaki, I. Takahashi, N. Ueta, Ethanolamine
618 plasmalogens protect cholesterol-rich liposomal membranes from
619 oxidation caused by free radicals. *Chem Phys Lipids* **120**, 145-151 (2002).
620 23. A. L. White, P. Modaff, F. Holland-Morris, R. M. Pauli, Natural history of
621 rhizomelic chondrodysplasia punctata. *Am J Med Genet A* **118a**, 332-342
622 (2003).
623 24. V. Gonzalez-Covarrubias *et al.*, Lipidomics of familial longevity. *Aging Cell*
624 **12**, 426-434 (2013).
625 25. I. Pradas *et al.*, Exceptional human longevity is associated with a specific
626 plasma phenotype of ether lipids. *Redox biology* **21**, 101127 (2019).
627 26. M. K. Ghosh, A. K. Hajra, Subcellular distribution and properties of
628 acyl/alkyl dihydroxyacetone phosphate reductase in rodent livers. *Archives*
629 *of biochemistry and biophysics* **245**, 523-530 (1986).
630 27. D. Hardeman, H. Van den Bosch, Topography of ether phospholipid
631 biosynthesis. *Biochimica et Biophysica Acta (BBA)-Lipids and Lipid*
632 *Metabolism* **1006**, 1-8 (1989).
633 28. H. Singh, K. Beckman, A. Poulos, Exclusive localization in peroxisomes of
634 dihydroxyacetone phosphate acyltransferase and alkyl-dihydroxyacetone
635 phosphate synthase in rat liver. *Journal of lipid research* **34**, 467-477
636 (1993).
637 29. R. Hua *et al.*, VAPs and ACBD5 tether peroxisomes to the ER for
638 peroxisome maintenance and lipid homeostasis. *Journal of Cell Biology*
639 **216**, 367-377 (2017).
640 30. X. Shi *et al.*, A Caenorhabditis elegans model for ether lipid biosynthesis
641 and function. *Journal of lipid research* **57**, 265-275 (2016).
642 31. D. I. Benjamin *et al.*, Ether lipid generating enzyme AGPS alters the
643 balance of structural and signaling lipids to fuel cancer pathogenicity. *Proc*
644 *Natl Acad Sci U S A* **110**, 14912-14917 (2013).
645 32. Y. Sogame, A. Kitamura, M. Yabuki, S. Komuro, A comparison of uptake
646 of metformin and phenformin mediated by hOCT1 in human hepatocytes.
647 *Biopharm Drug Dispos* **30**, 476-484 (2009).
648 33. E. D. Segal *et al.*, Relevance of the OCT1 transporter to the antineoplastic
649 effect of biguanides. *Biochem Biophys Res Commun* **414**, 694-699 (2011).
650 34. C. L. Perez, M. R. Van Gilst, A 13C isotope labeling strategy reveals the
651 influence of insulin signaling on lipogenesis in C. elegans. *Cell Metab* **8**,
652 266-274 (2008).
653 35. M. A. Perez, J. L. Watts, Worms, Fat, and Death: Caenorhabditis elegans
654 Lipid Metabolites Regulate Cell Death. *Metabolites* **11** (2021).

655 36. R. J. Shmookler Reis *et al.*, Modulation of lipid biosynthesis contributes to
656 stress resistance and longevity of C. elegans mutants. *Aging (Albany NY)*
657 **3**, 125-147 (2011).
658 37. M. Horikawa, T. Nomura, T. Hashimoto, K. Sakamoto, Elongation and
659 desaturation of fatty acids are critical in growth, lipid metabolism and
660 ontogeny of Caenorhabditis elegans. *J Biochem* **144**, 149-158 (2008).
661 38. J. Apfeld, G. O'Connor, T. McDonagh, P. S. DiStefano, R. Curtis, The
662 AMP-activated protein kinase AAK-2 links energy levels and insulin-like
663 signals to lifespan in C. elegans. *Genes Dev* **18**, 3004-3009 (2004).
664 39. R. Curtis, G. O'Connor, P. S. DiStefano, Aging networks in Caenorhabditis
665 elegans: AMP-activated protein kinase (aak-2) links multiple aging and
666 metabolism pathways. *Aging Cell* **5**, 119-126 (2006).
667 40. M. M. Senchuk *et al.*, Activation of DAF-16/FOXO by reactive oxygen
668 species contributes to longevity in long-lived mitochondrial mutants in
669 Caenorhabditis elegans. *PLoS Genet* **14**, e1007268 (2018).
670 41. M. A. Schreiber, J. T. Pierce-Shimomura, S. Chan, D. Parry, S. L.
671 McIntire, Manipulation of behavioral decline in Caenorhabditis elegans
672 with the Rag GTPase raga-1. *PLoS Genet* **6**, e1000972 (2010).
673 42. C. Kenyon, J. Chang, E. Gensch, A. Rudner, R. Tabtiang, A C. elegans
674 mutant that lives twice as long as wild type. *Nature* **366**, 461-464 (1993).
675 43. N. Braverman *et al.*, Human PEX7 encodes the peroxisomal PTS2
676 receptor and is responsible for rhizomelic chondrodysplasia punctata.
677 *Nature genetics* **15**, 369-376 (1997).
678 44. A. M. Motley *et al.*, Rhizomelic chondrodysplasia punctata is a
679 peroxisomal protein targeting disease caused by a non-functional PTS2
680 receptor. *Nature genetics* **15**, 377-380 (1997).
681 45. P. E. Purdue, J. W. Zhang, M. Skoneczny, P. B. Lazarow, Rhizomelic
682 chondrodysplasia punctata is caused by deficiency of human PEX7, a
683 homologue of the yeast PTS2 receptor. *Nature genetics* **15**, 381-384
684 (1997).
685 46. B. Itzkovitz *et al.*, Functional characterization of novel mutations in GNPAT
686 and AGPS, causing rhizomelic chondrodysplasia punctata (RCDP) types 2
687 and 3. *Hum Mutat* **33**, 189-197 (2012).
688 47. M. O. Grimm *et al.*, From brain to food: analysis of phosphatidylcholins,
689 lyso-phosphatidylcholins and phosphatidylcholin-plasmalogens derivates
690 in Alzheimer's disease human post mortem brains and mice model via
691 mass spectrometry. *J Chromatogr A* **1218**, 7713-7722 (2011).
692 48. D. B. Goodenowe *et al.*, Peripheral ethanolamine plasmalogen deficiency:
693 a logical causative factor in Alzheimer's disease and dementia. *J Lipid Res*
694 **48**, 2485-2498 (2007).
695 49. X. Han, D. M. Holtzman, D. W. McKeel, Jr., Plasmalogen deficiency in
696 early Alzheimer's disease subjects and in animal models: molecular
697 characterization using electrospray ionization mass spectrometry. *J*
698 *Neurochem* **77**, 1168-1180 (2001).

699 50. Y. Zou *et al.*, Plasticity of ether lipids promotes ferroptosis susceptibility
700 and evasion. *Nature* **585**, 603-608 (2020).
701 51. D. H. Albert, C. E. Anderson, Ether-linked glycerolipids in human brain
702 tumors. *Lipids* **12**, 188-192 (1977).
703 52. F. Snyder, R. Wood, Alkyl and alk-1-enyl ethers of glycerol in lipids from
704 normal and neoplastic human tissues. *Cancer Res* **29**, 251-257 (1969).
705 53. P. A. Jaffrès *et al.*, Alkyl ether lipids, ion channels and lipid raft
706 reorganization in cancer therapy. *Pharmacol Ther* **165**, 114-131 (2016).
707 54. G. Arthur, R. Bittman, Glycosylated antitumor ether lipids: activity and
708 mechanism of action. *Anticancer Agents Med Chem* **14**, 592-606 (2014).
709 55. T. W. Mitchell, R. Buffenstein, A. J. Hulbert, Membrane phospholipid
710 composition may contribute to exceptional longevity of the naked mole-rat
711 (Heterocephalus glaber): a comparative study using shotgun lipidomics.
712 *Exp Gerontol* **42**, 1053-1062 (2007).
713 56. D. Munro, P. U. Blier, The extreme longevity of Arctica islandica is
714 associated with increased peroxidation resistance in mitochondrial
715 membranes. *Aging Cell* **11**, 845-855 (2012).
716 57. M. Honsho, S. Asaoku, Y. Fujiki, Posttranslational regulation of fatty acyl-
717 CoA reductase 1, Far1, controls ether glycerophospholipid synthesis.
718 *Journal of Biological Chemistry* **285**, 8537-8542 (2010).
719 58. A. A. Soukas, E. A. Kane, C. E. Carr, J. A. Melo, G. Ruvkun,
720 Rictor/TORC2 regulates fat metabolism, feeding, growth, and life span in
721 Caenorhabditis elegans. *Genes & development* **23**, 496-511 (2009).
722 59. S. K. Han *et al.*, OASIS 2: online application for survival analysis 2 with
723 features for the analysis of maximal lifespan and healthspan in aging
724 research. *Oncotarget* **7**, 56147-56152 (2016).
725 60. R. S. Kamath, J. Ahringer, Genome-wide RNAi screening in
726 Caenorhabditis elegans. *Methods* **30**, 313-321 (2003).
727 61. E. C. Pino, A. A. Soukas, Quantitative Profiling of Lipid Species in
728 Caenorhabditis elegans with Gas Chromatography-Mass Spectrometry.
729 *Methods Mol Biol* **2144**, 111-123 (2020).
730 62. E. C. Pino, C. M. Webster, C. E. Carr, A. A. Soukas, Biochemical and high
731 throughput microscopic assessment of fat mass in Caenorhabditis
732 elegans. *J Vis Exp* 10.3791/50180 (2013).

733 **Figures and Tables**

734

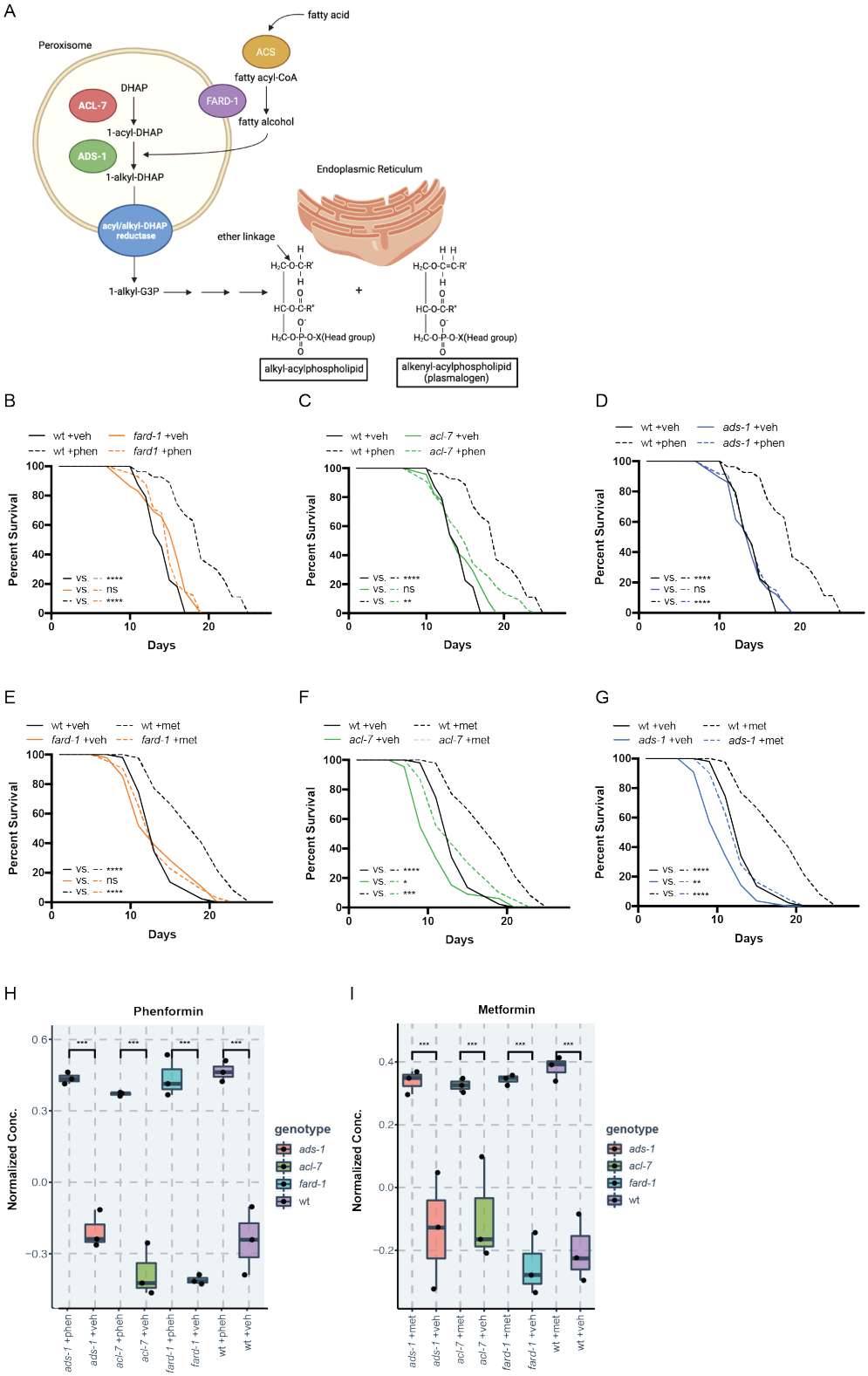

735

736 **Figure 1. Genes responsible for ether lipid biosynthesis are necessary for**

737 **biguanide-induced lifespan extension.** Ether lipid synthesis is catalyzed by
738 three enzymes: fatty acyl reductase FARD-1, acyltransferase ACL-7 and
739 alkylglycerone phosphate synthase ADS-1 (*A*). The latter two are localized to the
740 peroxisomal lumen. *Missense* mutations in *fard-1* (*B*), acl-7 (*C*), and *ads-1* (*D*) in
741 *C. elegans* suppress phenformin-induced lifespan extension. A deficiency of ether
742 lipid synthesis in *fard-1* (*E*), *acl-7* (*F*), and *ads-1* (*G*) worm mutants blunts
743 metformin-induced lifespan extension. Results are representative of 3 biological
744 replicates. *, $P < 0.05$; **, $P < 0.01$; ***, $P < 0.001$; ****, $P < 0.0001$ by log-rank
745 analysis. See also Figure S1 and refer to Dataset S1 for tabular survival data and
746 biological replicates. Normalized concentrations of phenformin (*H*) and metformin
747 (*I*) in vehicle, 4.5mM phenformin, or 50 mM metformin treated wild type *C. elegans*
748 versus *fard-1*, *acl-7*, and *ads-1* mutants. n= 3 biological replicates; ***, $P < 0.001$
749 by two-tailed students *t*-test. Box represents $75^{th}/25^{th}$ percentiles, while whisker
750 represents higher/lower hinge +/- [1.5 * interquartile range (IQR)].

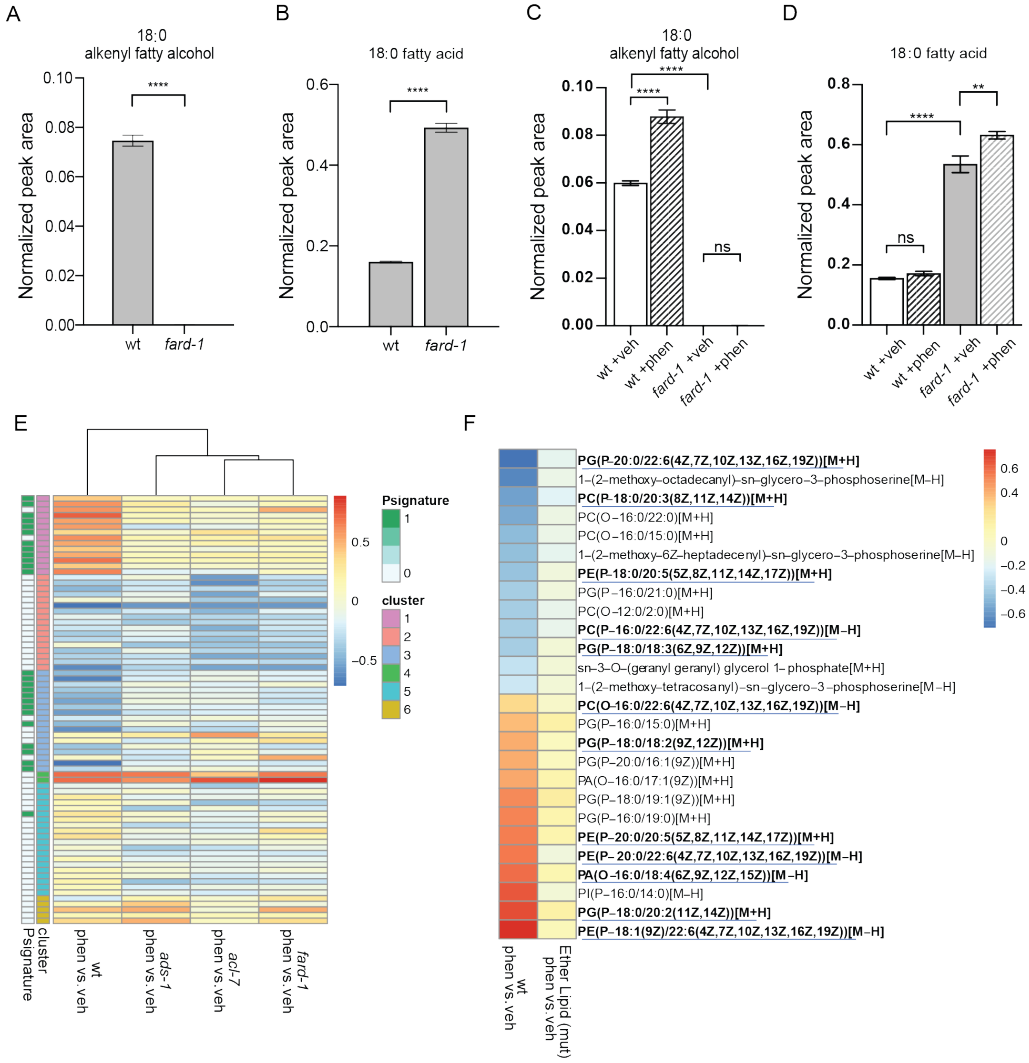

Figure 2. Phenformin induces an ether lipid metabolite signature that is blunted in ether lipid biosynthesis mutants. Loss-of-function *fard-1* mutants have significant reduction in 18:0 fatty alcohol derivatized from 18-carbon containing alkenyl ether lipids (also known as plasmalogens) by GC/MS (*A*) and corresponding accumulation of the fatty acid stearate (18:0, *B*). Wild type worms treated with 4.5 mM phenformin display a significant increase in 18:0 fatty alcohol derivatized from alkenyl ether lipids relative to vehicle control, with levels remaining essentially undetectable in *fard-1* mutants on vehicle or drug (*C*). Phenformin 4.5mM treatment does not impact stearate levels in wild type worms, however it does result in a greater accumulation of stearate in *fard-1* mutants (*D*). For *A-D*, **, $P < 0.01$; ****, $P < 0.0001$, by two-way ANOVA, n = 3 biological replicates. Cluster analysis of ether lipids significantly altered in response to phenformin (*E*). Cluster 1 denotes a set of ether lipids that increased significantly in phenformin treated wild type worms but are unaffected in ether lipid mutants *fard-1*, *acl-7* and *ads-1*. Cluster 3 represents a set of ether lipids that decreased significantly in phenformin treated wild type worms but unaffected in ether lipid mutants. n=3 biological replicates; adj. *P*-value < 0.05. See Table S2 and S3 for raw mass

769 spectrometry data and identity of metabolites in clusters, respectively. Heat map
770 of 26 ether lipids identified by linear modeling with significant fold change in
771 abundance between vehicle and 4.5mM phenformin treatment in the wildtype
772 background that do not show significant differences between vehicle and drug
773 treated ether lipid deficient mutant (*F*). 10 of 13 ether lipids increased in abundance
774 are alkenyl-type (plasmalogen, indicated by "P" in their name prior to the fatty
775 alcohol designation) ether lipids, versus alkyl-type (indicated by "O" in their name
776 prior to fatty alcohol designation). Twelve ether lipids (bold and underlined) harbor
777 very long chain polyunsaturated fatty acids at the sn-2 position. n=3 biological
778 replicates; adj. $P<0.05$. PG, phosphatidyl glycerol; PE phosphatidyl ethanolamine;
779 PC phosphatidyl choline; PI, phosphatidyl inositol; PA, phosphatidic acid.
780

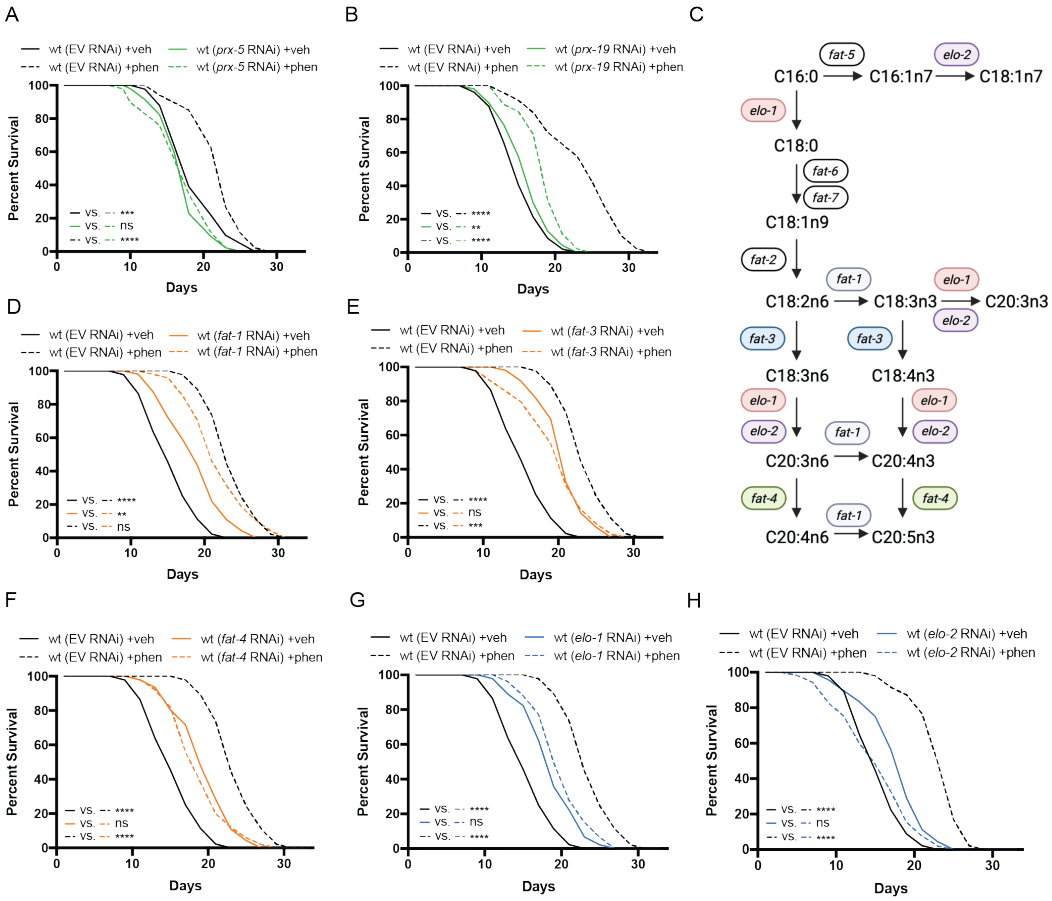

Figure 3. Fatty acid elongases and desaturases are required **for the prolongevity effects of biguanides.** Knockdown of *prx-5* (*A*) and *prx-19* (*B*) by RNAi significantly suppresses phenformin-mediated lifespan extension. Schematic representation of the polyunsaturated fatty acid (PUFA) synthesis pathway in *C. elegans* (*C*). RNAi of three fatty acid desaturases (*D-F*) and two fatty acid elongases (*G* and *H*) involved in the synthesis of 18- and 20-carbon polyunsaturated fatty acids blunt phenformin-mediated lifespan extension in wild type worms. For *A, B* and *D-H,* results are representative of 2-3 biological replicates. **, $P < 0.01$; ***, $P < 0.001$; ****, $P < 0.0001$ by log-rank analysis; see also Dataset S1 for tabular survival data and biological replicates.

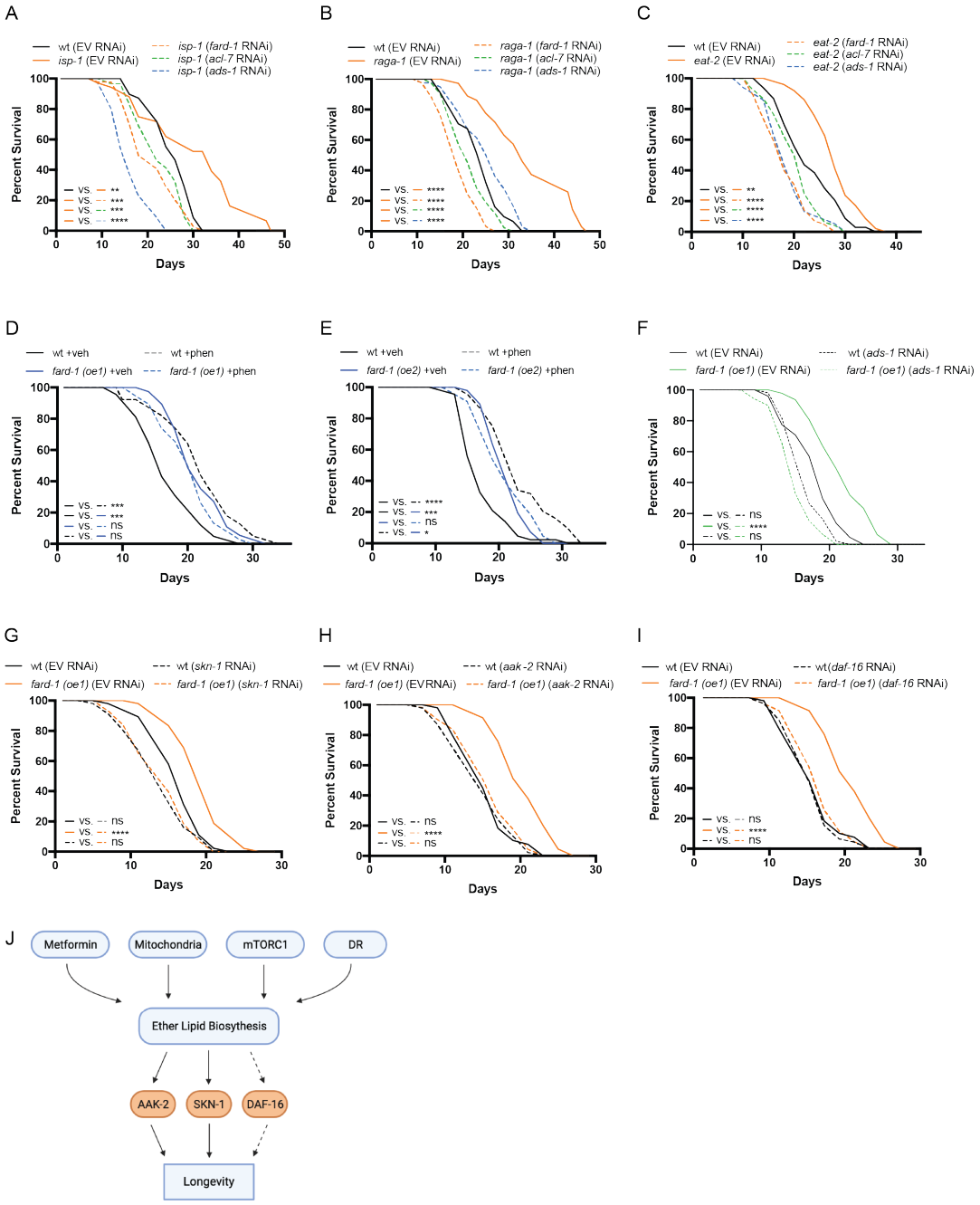

Figure 4. Genes involved in ether lipid biosynthesis are required in multiple longevity paradigms and FARD-1 overexpression is sufficient to extend lifespan. *isp-1*, *raga-1*, and *eat-2* mutants display extended lifespan relative to wild type animals that is suppressed by knockdown of any of the three members of the ether lipid biosynthetic pathway (*A-C*). Two independently-generated *fard-1* overexpression (oe) transgenic strains exhibit lifespan extension that is not further extended by concomitant phenformin treatment (*D-E*). RNAi knockdown of *ads-1* suppresses *fard-1* (oe) lifespan extension, indicating that the *fard-1* (oe)-mediated lifespan extension is dependent upon ether lipid synthesis (*F*). RNAi of *skn-1* (*G*), *aak-2* (*H*), and *daf-16* (*I*) suppress *fard-1* (oe)-mediated lifespan extension. For *A-*

804 *I*, results are representative of 2-3 biological replicates. *, $P < 0.05$, **, $P < 0.01$;
805 ***, $P < 0.001$; ****, $P < 0.0001$ by log-rank analysis. See also Figure S3 and
806 Dataset S1 for tabular survival data and biological replicates. Model for the role of
807 the ether lipid biosynthetic machinery in biguanide-mediated lifespan extension (*J*).